

# Olympic Ring Formation from Newly Prepared Barium Hexaferrite Nanoparticle Suspension

Kurikka V. P. M. Shafi,<sup>†</sup> Israel Felner,<sup>‡</sup> Y. Mastai,<sup>§</sup> and Aharon Gedanken<sup>\*,†</sup>

Department of Chemistry, Bar-Ilan University, Ramat-Gan 52900, Israel, Racah Institute of Physics, Hebrew University of Jerusalem, Jerusalem, Israel, and Department of Materials and Interface, Weizmann Institute of Science, Rehovot, 76100, Israel

Received: December 9, 1998; In Final Form: February 23, 1999

We report here, the first observation of features such as the *Olympic Rings* on transmission electron micrographs of amorphous BaFe<sub>12</sub>O<sub>19</sub> nanoparticles prepared by a sonochemical decomposition technique. The barium hexaferrite was formed as a colloidal solution without the use of a surfactant. Rings of smaller dimensions trapped inside the larger ones was another unique observation. The intersection of two rings is amazing, as this is in direct contradiction to the proposed mechanism for the ring formation, based on the dry hole formation on an evaporating thin film completely wetted to the substrate. The creation of this unique feature is attributed to the interplay of magnetic forces with the regular particle–substrate interactions.

## Introduction

Hexagonal magnetic hard ferrites such as BaFe<sub>12</sub>O<sub>19</sub> are of great scientific and technological importance. Owing to their large crystalline anisotropy and high intrinsic coercivity, they are used in the production of permanent magnets and in the fabrication of certain microwave devices. Fine particles of BaFe<sub>12</sub>O<sub>19</sub> are currently used in high-density perpendicular magnetic recording media. A wide range of methods has been used to prepare ultrafine ferrite particles, including chemical coprecipitation,<sup>1</sup> combustion,<sup>2</sup> pyrosol,<sup>3</sup> and sol–gel<sup>4</sup> methods, as well as microemulsion<sup>5</sup> and glass crystallization<sup>6</sup> techniques. Apart from the citrate precursor (sol–gel) method, in all these methods, formation of single-phase BaFe<sub>12</sub>O<sub>19</sub> takes place at 900 °C or above, and the particles obtained are of relatively larger size, >50 nm. Control over the size of the particles and their uniformity, purity, and good crystallinity is the major difficulty in these synthetic methods. We have utilized ultrasonic irradiation to achieve, at the atomic level, mixing of the constituent ions in the required stoichiometric ratio. In this paper we present a new method for the preparation of BaFe<sub>12</sub>O<sub>19</sub>. The as-prepared material was formed in the amorphous state. We also report on the formation of nanorings and intersecting nanorings when the solution of the amorphous as-prepared material was left to dry on a Formavar grid and examined by transmission electron microscopy.

## Experimental and Results

**(a) Synthesis of Material.** A few examples have been recently presented for the use of ultrasonic radiation in the formation of colloidal solutions.<sup>10–12</sup> In these cases a surfactant such as oleic acid was introduced to assist in the formation of the colloidal solution. In the current procedure no surfactant was required to form the colloidal solution.

A solution of Fe(CO)<sub>5</sub> and barium ethylhexanoate (Ba-[OOCCH(C<sub>2</sub>H<sub>5</sub>)C<sub>4</sub>H<sub>9</sub>]<sub>2</sub>) in decane, in stoichiometric ratio, was

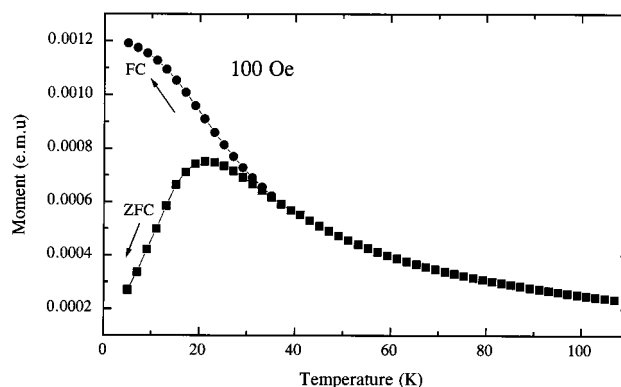


**Figure 1.** Temperature-dependent, field-cooled (FC), and zero-field-cooled (ZFC) magnetic curve of the amorphous sample, measured in a dc field of 100 Oe.

decomposed by high-intensity ultrasonication, employing a direct immersion titanium horn (Vibracell, 20 kHz, 100 W/cm<sup>2</sup>) in the solution beaker to obtain the product. The as-prepared material was an amorphous BaFe<sub>12</sub>O<sub>19</sub> precursor in colloidal suspension, where the particles are in the nanometer size regime and are homogeneously distributed. The precursor is extracted from the solution as powder by precipitation or by evaporation and then calcined at low temperature (600 °C) to obtain the final BaFe<sub>12</sub>O<sub>19</sub> crystalline nanosized powders. The EDX profile of the amorphous as-prepared precursor powder showed that the Ba and Fe are in stoichiometric ratio, as in BaFe<sub>12</sub>O<sub>19</sub>. The XRD pattern of the final calcined, nanosized powder confirmed the presence of single-phase BaFe<sub>12</sub>O<sub>19</sub>, with no iron oxide impurities present.

**(b) Magnetic Properties.** The amorphous as-prepared particles are found to be superparamagnetic in nature. Figure 1 shows the temperature-dependent field-cooled (FC) and zero-field-cooled (ZFC) magnetic susceptibility curves of the amorphous sample, measured in a dc field of 100 Oe. ZFC shows a sharp maximum which is characteristic of a spin-glass type material. The superparamagnetic particles show a blocking temperature of 25 K, defined as the maximum in the ZFC curve.<sup>13</sup> The broad susceptibility indicates the distribution of

\* Author to whom correspondence should be addressed.

<sup>†</sup> Bar-Ilan University.

<sup>‡</sup> Hebrew University of Jerusalem.

<sup>§</sup> Weizmann Institute of Science.

the particle size. Irreversibility occurs below 35 K. The blocking temperature and the measurement time constants are consistent with the magnetic particle diameter of 5 nm.<sup>13</sup>

**(c) Ring Formation.** Ring formation of macroscopic particles (e.g., stains from coffee, tomato bits, etc.) is common. However, the formation of macroscopic rings from mesoscopic particles (e.g., polyballs) is not common, and is being studied both experimentally and theoretically.<sup>7,8</sup> Ohara et al.<sup>9</sup> discuss the dry hole formation on the wetting layers of very thin films, formed by the evaporation of a drop of solution of silver nanoparticle in hexane on an amorphous carbon substrate. They observed an array, consisting of a ring (0.9  $\mu\text{m}$  diameter) of close packed Ag nanoparticles of 2.5 nm size, formed upon the pinning to the substrate of the perimeter (the contact line between fluid and substrate) of a growing hole that has nucleated in a sufficiently thin film of dilute solutions of particles. The concentration of the particles inside the ring is smaller than the concentration of particles outside. This was consistent with their belief that the rings are formed due to holes opening up in the liquid film on drying, and pushing the particles into the rims. They correlate the formation of rings with the presence of monodisperse larger particles, whereas the greater number of smaller particles with polydispersity will give compact size-aggregated domains. Ring formation is explained by the size-dependent interaction between the particles and the substrate.

Although our studies are technically similar to those of Ohara et al.,<sup>9</sup> the results are different. One drop of a suspension of amorphous  $\text{BaFe}_{12}\text{O}_{19}$  precursor in decane was placed on a carbon-coated Formvar copper grid (diam = 3 mm) and allowed to evaporate. The evaporation took place at ambient temperature (24  $^{\circ}\text{C}$ ) and at a 30% humidity. A transmission electron micrograph (Figure 2) revealed an array of rings of diameter about 600 nm that is much smaller than the ring reported by Ohara et al. and other 3D rings reported elsewhere.<sup>7</sup> The surface coverage of these rings was more than 50% and the annular width is about 25 nm. The selected area electron diffraction (SAED) pattern of the annular region shows the particles are indeed amorphous, aggregated, and without any ordered structures. The rings were formed successively on drying the films. On the first day, only the pure rings were observed (Figure 2), while the trapped rings and the intersecting rings (Figure 3) appeared on the next day. A closer look at the TEM picture shows that the particles inside and outside the rings are in uniform concentration which is very different from what was observed by Ohara et al. Moreover, the TEM picture of another specimen (Figure 3) shows interesting features. Here, one can see the intersecting rings forming the so-called *Olympic Rings*. Rings of various sizes at various stages of growth and with different annular width (10 nm) can be seen on another micrograph, Figure 4. Also rings of smaller dimensions are seen trapped inside the larger ones. When the grid planes were photographed at different inclinations, the same TEM images were observed. We could not distinguish between pictures taken at different angles between the grid and the electron beam. This indicates that the intersection region is aligned in the same plane (within the 25 nm of the annular width). It is amazing to see the intersection of two rings, as this is in direct contradiction to the proposed mechanism for the ring formation, based on the dry hole formation on an evaporating thin film completely wetted to the substrate. Hole nucleation occurs in *nonvolatile* wetting fluids, where the film becomes unstable at a thickness  $t$  below a critical value  $t_{\text{hole}}$ .<sup>14</sup> The hole opens up to restore the film to its equilibrium thickness  $t_e$  which is given by  $(3A_H/S)^{1/2}$ , where  $A_H = A_{\text{sl}} - A_{\text{ll}} > 0$  is the Hamaker constant.<sup>10</sup>  $S$ , the

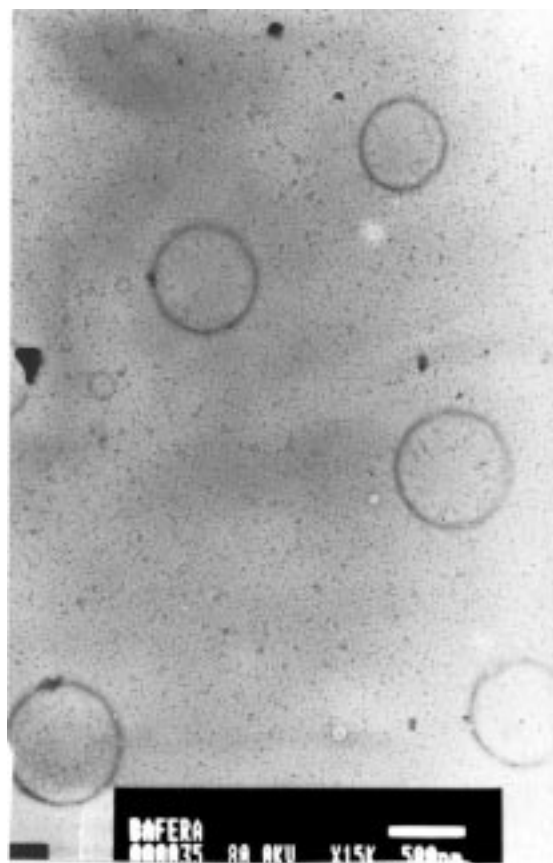


**Figure 2.** TEM micrograph showing the self-organization of superparamagnetic nanoparticles into submicron size (600 nm) rings. The rings are of near uniform size with an annular width of about 25 nm. The scale bar shown is 500 nm.

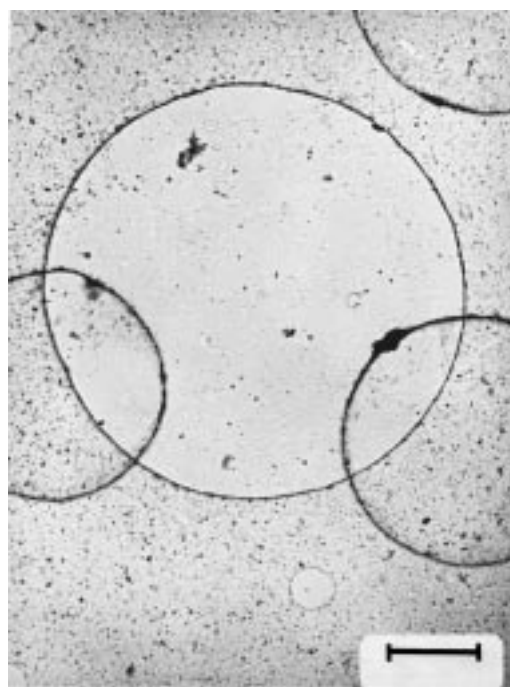


**Figure 3.** TEM micrograph showing rings of various sizes. The rings seem to intersect each other forming the so-called *Olympic Rings*. The scale bar is 0.7  $\mu\text{m}$ .

positive spreading coefficient, is defined as  $S = \gamma_{\text{sv}} - (\gamma_{\text{sl}} + \gamma)$ , where  $\gamma$  is the liquid–vapor interfacial tension and  $\gamma_{\text{sv}}$  ( $\gamma_{\text{sl}}$ ) is solid–vapor (solid–liquid) interfacial surface tension. Ne-

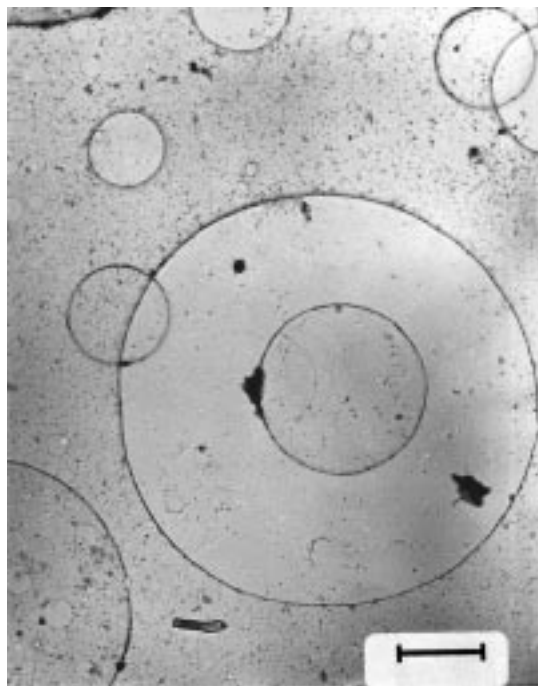


**Figure 4.** TEM micrograph showing rings at various stages of growth. Rings of smaller dimensions are seen trapped inside the larger one. The annular width of the ring is about 10 nm. The scale bar is 1  $\mu\text{m}$ .

glecting hydrodynamic effects, the force acting on the rim of a hole of radius  $R$  can be simplified as  $2\pi RS[t_e^2/t_{\text{hole}}^2 - 1]$ .<sup>9,15</sup> The particle can move along with the expanding rim only if the force opening the hole is strong enough to overcome the static friction arising from particle–substrate and particle–particle interactions. The rim will be pinned when the hole radius reaches a value  $R_{\text{pin}}$  which is determined by the balance between the lateral frictional force and the outward thickening force, given below<sup>9</sup>

$$F_{z,\text{disp}} K \approx 2\pi r^2 S [(t_e/t_{\text{hole}})^2 - 1] / \phi R_{\text{pin}}$$

where  $F_{z,\text{disp}}$ <sup>16</sup> is the downward dispersional force attracting an individual particle to the substrate,  $K$  is the friction coefficient, and  $\phi$  is the area fraction of the surface covered by the particles (of individual radius  $r$ ) in the uniform wetting layer before the nucleation of any holes. Thus, for a specific particle size  $r$ , solvent, and substrate (i.e., for a fixed set of values of  $S$ ,  $t_e$ , and  $t_{\text{hole}}$ ), the ring size  $R_{\text{pin}}$  from the above equation will vary inversely with surface coverage of the particle of radius  $r$ . Provided the size distribution is narrow, for a given  $\phi$ , all rings should be of the same size.

The above arguments are valid for a well-defined nanocrystalline particle system, where the downward dispersional force,  $F_{z,\text{disp}}$ , depends only on the individual particle sizes. In our system, where the particles are agglomerated, the interparticle interactions play an important role. The intersection of the rings

of various pinning radii,  $R_{\text{pin}}$ , and the trapping of the smaller ring inside the larger one, cannot be explained by the proposed model of a single wetting layer.

We believe that for  $\text{BaFe}_{12}\text{O}_{19}$  magnetic forces play an important role in the ring formation. Self-organization of nanoparticles is already known in the literature both on substrate and in solution. Both theoretical and experimental studies have been carried out on monodisperse nanocrystalline particles of metals,<sup>18,19</sup> sulfide,<sup>20</sup> and semiconductors<sup>21</sup> on the formation of ordered arrays of nanocrystal superlattices. Chain formation of ferromagnetic nanoparticles as well as the growth into acicular shape, both in the presence and absence of a magnetic field, is well-known.<sup>22</sup> These authors have observed the self-organization of amorphous cobalt nanoparticles to an acicular form in a surfactant-stabilized colloidal solution on aging at ambient conditions.<sup>11</sup> The magnetic dipolar interactions is the key factor in producing such effects, and the ring formation is an ideal condition for an energetically most favored state. In a solution, such an ideal situation can be ruled out because of kinetic factors. However, the whole scenario can be different when a drop of this solution is put on a carbon grid. As the drop evaporates to become a thin film, the magnetic particles are anchored on the substrate due to particle–support interactions. The interparticle dipolar interactions can outweigh the particle–support interactions leading to the formation of rings.

## References and Notes

- (1) Popov, O. J. *Magn. Magn. Mater.* **1991**, 99, 119.
- (2) Castro, S. J. *Magn. Magn. Mater.* **1996**, 152, 61.
- (3) Kaczmarek, W. A.; Ninham, B. W.; Calka, A. *J. Appl. Phys.* **1991**, 70, 5909.
- (4) Sankaranarayanan, V.; Khan, D. C. *J. Magn. Magn. Mater.* **1996**, 153, 337.
- (5) Pillai, V.; Kumar, P.; Multani, M. S.; Shah, D. O. *Colloids Surf., A* **1993**, 80, 69.
- (6) Pfeiffer, H.; Chantrell, R. W.; Gornet, P.; Schuppel, W.; Sinn, E.; Rosler, M. *J. Magn. Magn. Mater.* **1993**, 125, 373.
- (7) Adachi, E.; Dimitrov, A. S.; Nagayama, K. *Langmuir* **1995**, 11, 1057.
- (8) Elbaum, M.; Lipson, S. G. *Phys. Rev. Lett.* **1994**, 72, 3562.
- (9) Ohara, P. C.; Heath, J. R.; Gelbart, W. G. *Ang. Chem., Int. Ed. Engl.* **1997**, 36, 1078.
- (10) Suslick, K. S.; Feng, M.; Heyon, T. *J. Am. Chem. Soc.* **1996**, 118, 11960.
- (11) Shafi, K. V. P. M.; Gedanken, A.; Prozorov, R. *Adv. Mater.* **1998**, 10, 590.
- (12) Shafi, K. V. P. M.; Wize, S.; Prozorov, T.; Gedanken, A. *Thin Solid Films* **1998**, 318, 38.
- (13) Morup, S. *Europhys. Lett.* **1994**, 28, 671.
- (14) Brochard-Wyart, F.; di Meglio, J.-M.; Quere, D.; de Gennes, P.-G. *Langmuir* **1991**, 7, 335.
- (15) Brochard-Wyart, F.; Daillant, J. *Can. J. Phys.* **1990**, 68, 1084.
- (16) Safran, S. A. *Statistical Thermodynamics of Surface, Interface, and Membranes*; Addison-Wesley: Reading, MA, 1994, and reference therein.
- (17) Morup, S. *Europhys. Lett.* **1994**, 28, 671.
- (18) Heath, J. R.; Knobler, C. M.; Leff, D. V. *J. Phys. Chem. B* **1997**, 101, 189.
- (19) Taleb, A.; Petit, C.; Pileni, M. P. *Chem. Mater.* **1997**, 9, 950.
- (20) Motte, L.; Biloudet, F.; Lacaze, E.; Douin, J.; Pileni, M. P. *J. Phys. Chem.* **1997**, 101, 138.
- (21) Murray, C. B.; Kagan, C. R.; Bawendi, M. G. *Science* **1995**, 270, 1335.
- (22) Chen, J.; Nikles, D. E. *IEEE Trans. Magn.* **1996**, 32, 4478.